DOI: 10.1002/ejic.200500731

Two New Cu^{II} Coordination Polymers: Studies of Topological Networks and Water Clusters

Jin Yang,[a] Jian-Fang Ma,*[a] Ying-Ying Liu,[a] Ji-Cheng Ma,[a] Heng-Qing Jia,[b] and Ning-Hai Hu[b]

Keywords: Coordination polymers / Copper / Materials science / Topology / Water clusters

Two new Cu^{II} coordination polymers, namely $[Cu_2(BDC)_2(L)_4(H_2O)_2]\cdot 14H_2O$ (**1**) and $[Cu_{1.5}(BTC)(L)_{1.5}(H_2O)_{0.5}]\cdot 2H_2O$ (**2**), where L = 1,1′-(1,4-butanediyl)bis(imidazole), BDC = 1,4-benzenedicarboxylate, and BTC = 1,3,5-benzenetricarboxylate, have been synthesized at room temperature. Complex **1** exhibits an unusual, square-planar, four-connected 2D ${}^{2}_{6}4$ net, which has been predicated by Wells. Interestingly, three types of water clusters, namely $(H_2O)_6$, $(H_2O)_8$, and $(H_2O)_{10}$, are observed in the hydrogen-bonded layers constructed by the BDC ligands and water molecules. The BTC anion in compound **2** is coordinated to the Cu^{II} cation as tetradentate ligand to form a $(6^6)_2(4^26^48^4)_2(6^48 10)$ net containing three kinds of nonequivalent points. Thermogravimetric analyses (TGA) and IR spectra for **1** and **2** are also discussed in detail. (© Wiley-VCH Verlag GmbH & Co. KGaA, 69451 Weinheim, Germany, 2006)

Introduction

During the past few years much attention has been paid to theoretical and experimental studies of small water clusters due to their unusual properties and importance in many physical, chemical, and biological processes.[1] A detailed understanding of the numerous possible structures and stabilities of isolated water clusters in diverse surroundings can help us study the nature of water–water interactions in bulk water or ice.[2] For example, the water hexamer is the building block of ice I_h and appears to be relevant to liquid water as well.[3] Several different isomers for the water hexamer, such as book, bag, ring, cage, and prism topologies, have been found from theoretical calculations.[4] Thus, the search for experimental models of these small water clusters is very important to improve our study of the structures and characteristics of liquid water and ice.

On the other hand, understanding the structure of coordination polymers is an important aspect to achieve a true advance in the synthesis and design of new materials for practical applications.[5] The analysis of network topology is a particularly useful tool for reducing multidimensional structures to simple node-and-connection reference nets. Wells has listed a large number of topologies in his classic monographs on networks,[6] and numerous fascinating archetypal structures, including diamond (6^6), SiO_2 (6^48^2-b), $SrSi_2$ (10^3-a), α-$ThSi_2$ (10^3-b), and PtS (4^28^4) have been reported[7] that are of fundamental importance in structural design and in the understanding of structure–property correlations. In this work we report two new Cu^{II} coordination polymers, namely $[Cu_2(BDC)_2(L)_4(H_2O)_2]\cdot 14H_2O$ (**1**), which contains an unusual, square-planar, four-connected ${}^{2}_{6}4$ net and three types of water clusters, and $[Cu_{1.5}(BTC)(L)_{1.5}(H_2O)_{0.5}]\cdot 2H_2O$ (**2**), which possesses a $(6^6)_2(4^26^48^4)_2(6^48 10)$ net [L = 1,1′-(1,4-butanediyl)bis(imidazole),[8] BDC = 1,4-benzenedicarboxylate, BTC = 1,3,5-benzenetricarboxylate; Scheme 1].

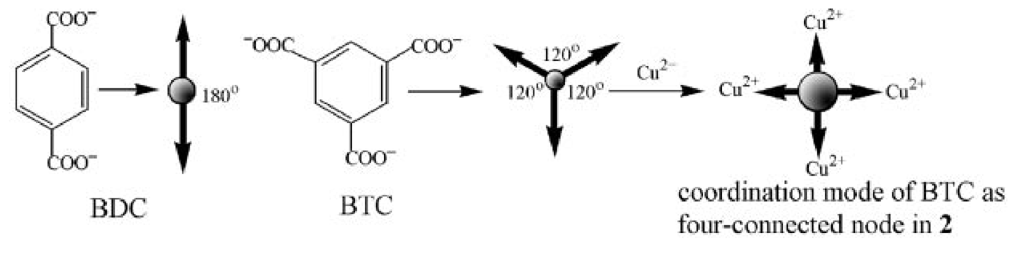

Scheme 1.

---

[a] Department of Chemistry, Northeast Normal University,
Changchun 130024, People's Republic of China
E-mail: jianfangma@yahoo.com.cn
Fax: +86-431-568-4009
[b] Changchun Institute of Applied Chemistry, Chinese Academy of Sciences,
Changchun 130022, People's Republic of China

Supporting information for this article is available on the WWW under http://www.eurjic.org or from the author.

Results and Discussion

Crystal Structures

The synthesis of complexes **1** and **2** is described in the Experimental Section. Selected bond lengths and angles for compounds **1** and **2** are listed in Table 1. Part of the structure of $[Cu_2(L)_4(H_2O)_2]\cdot(BDC)_2\cdot 14H_2O$ (**1**) is shown in Figure 1 (a). There are two crystallographically unique Cu^{II} cations in the asymmetric unit. Each Cu^{II} cation adopts a distorted square-pyramidal geometry by coordinating to four nitrogen atoms from four L molecules and one water molecule. Four nitrogen atoms (N1, N5, N9, and N8A for Cu1; N4, N11, N13, and N16A for Cu2) form the base of the pyramid and one water molecule (Ow1 for Cu1; Ow2 for Cu2) occupies the apical position, with respective Cu–O distances of 2.380 and 2.464 Å. The BDC anion acts as a counter-anion and structure-directing reagent, indicating that the coordination of L to the Cu^{II} cation is stronger than that of the BDC anion in this case.

The structure of **1** consists of an unusual, 2D, square-planar, four-connected $^{2}_{6}4$ net, which has been predicated by Wells.[6] In this net the Cu^{II} cation acts as a four-connected node and L acts as the edge of every circuit (Figure 1, b). This $^{2}_{6}4$ net is entirely different from the square-planar four-connected (8^6) net first reported by Tong et al. and us, which was not mentioned by Wells.[5g,8c] It is well known that when square-planar, four-connected building blocks self-assemble into extended structures, 2D (4,4) square grids are favored.[9] This observation shows that formation of a $^{2}_{6}4$ net may be attributed to the effects of the flexible L and the BDC anion. Moreover, if two of the L molecules act as each of two opposite edges, a single L molecule acts as each of the other four edges, and every Cu^{II} cation can be seen as a three-connected node, the structure of **1** can be regarded as a 2D (6,3) network.

Table 1. Selected bond lengths [Å] and angles [°] for compounds **1** and **2**.

$[Cu_2(L)_4(H_2O)_2]\cdot(BDC)_2\cdot 14H_2O$ (**1**)[a]			
N(1)–Cu(1)	2.030(3)	N(4)–Cu(2)	2.026(3)
N(5)–Cu(1)	2.008(3)	N(8)–Cu(1)$^{\#1}$	1.991(3)
N(9)–Cu(1)	2.005(3)	N(11)–Cu(2)	1.990(3)
N(13)–Cu(2)	2.004(3)	N(16)–Cu(2)$^{\#2}$	1.985(3)
OW1–Cu(1)	2.380(3)		
N(8)$^{\#1}$–Cu(1)–N(9)	175.20(10)	N(8)$^{\#1}$–Cu(1)–N(5)	91.32(11)
N(9)–Cu(1)–N(5)	90.28(10)	N(8)$^{\#1}$–Cu(1)–N(1)	90.19(11)
N(9)–Cu(1)–N(1)	88.05(10)	N(5)–Cu(1)–N(1)	177.40(10)
N(8)$^{\#1}$–Cu(1)–OW1	88.63(10)	N(9)–Cu(1)–OW1	95.89(10)
N(5)–Cu(1)–OW1	90.21(11)	N(1)–Cu(1)–OW1	91.95(11)
N(16)$^{\#2}$–Cu(2)–N(11)	177.28(11)	N(16)$^{\#2}$–Cu(2)–N(13)	92.13(11)
N(11)–Cu(2)–N(13)	89.64(11)	N(16)$^{\#2}$–Cu(2)–N(4)	90.95(11)
N(11)–Cu(2)–N(4)	87.46(11)	N(13)–Cu(2)–N(4)	174.22(11)
$[Cu_{1.5}(BTC)(L)_{1.5}(H_2O)_{0.5}]\cdot 2H_2O$ (**2**)[b]			
N(1)–Cu(2)	1.978(4)	N(3)–Cu(1)	1.994(4)
O(1)–Cu(1)	1.952(3)	O(2)–Cu(1)$^{\#1}$	2.319(3)
O(3)–Cu(1)$^{\#2}$	2.014(3)	O(5)–Cu(2)	1.937(3)
OW1–Cu(2)	2.319(7)	Cu(1)–N(6)$^{\#3}$	1.966(4)
Cu(1)–O(3)$^{\#4}$	2.014(3)	Cu(1)–O(2)$^{\#1}$	2.319(3)
O(1)–Cu(1)–N(6)$^{\#3}$	94.02(17)	O(1)–Cu(1)–N(3)	86.14(16)
N(6)$^{\#3}$–Cu(1)–N(3)	173.90(18)	O(1)–Cu(1)–O(3)$^{\#4}$	159.37(14)
N(6)$^{\#3}$–Cu(1)–O(3)$^{\#4}$	90.98(16)	N(3)–Cu(1)–O(3)$^{\#4}$	86.81(15)
O(1)–Cu(1)–O(2)$^{\#1}$	107.78(14)	N(6)$^{\#3}$–Cu(1)–O(2)$^{\#1}$	94.97(16)
N(3)–Cu(1)–O(2)$^{\#1}$	90.78(15)	O(3)$^{\#4}$–Cu(1)–O(2)$^{\#1}$	91.67(13)
O(5)–Cu(2)–O(5)$^{\#5}$	178(2)	O(5)–Cu(2)–N(1)	88.33(16)
O(5)$^{\#5}$–Cu(2)–N(1)	91.87(16)	N(1)–Cu(2)–N(1)$^{\#5}$	168.7(3)
O(5)–Cu(2)–OW1	88.900(11)	N(1)–Cu(2)–OW1	95.67(14)

[a] Symmetry codes for **1**: $^{\#1}$ $-x + 1, -y, -z - 1$; $^{\#2}$ $-x, -y + 1, -z$.
[b] Symmetry codes for **2**: $^{\#1}$ $-x + 1.5, -y + 1.5, -z + 1$; $^{\#2}$ $x, y + 1, z$; $^{\#3}$ $x, -y + 1, z - 0.5$; $^{\#4}$ $x, y - 1, z$; $^{\#5}$ $-x + 1, y, -z + 1.5$.

In addition, a notable feature within complex **1** is the presence of three types of water clusters, namely $(H_2O)_6$, $(H_2O)_8$, and $(H_2O)_{10}$, in the hydrogen-bonded layer of BDC anions and water molecules (Figure 2, a). The hydrogen-bonding parameters are outlined in Table 2. Within the $(H_2O)_6$ cluster, two water molecules (OW2 and OW2A) act as two hydrogen-bond donors with OW4 and OW4A as hydrogen-bond acceptors to form a cyclic water tetramer (Figure 2, b).[10,11] Interestingly, the cyclic water tetramer is hydrogen-bonded to two neighboring free water molecules, OW6 and OW6A, yielding a water hexamer. Furthermore, the oxygen atoms O2, O2A, O5, O5A, O7, and O7A from the BDC ligands are involved in hydrogen bonds with water molecules OW4, OW4A, OW6, and OW6A to stabilize the $(H_2O)_6$ cluster. Within the $(H_2O)_{10}$ cluster, four water molecules (OW7, OW7A, OW16, and OW16A) act as both hydrogen-bond donors and acceptors (Figure 2, c). Four water molecules (OW13, OW13A, OW15, and OW15A) play the role of hydrogen-bond donors, while another two water molecules (OW14 and OW14A) only act as hydrogen-bond acceptors. Four water molecules (OW15, OW15A, OW16, and OW16A) form a cyclic water tetramer through hydrogen bonds, which is further hydrogen-bonded by water molecules OW7, OW13, OW14, OW7A, OW13A, and OW14A, leading to an $(H_2O)_{10}$ cluster. Moreover, the $(H_2O)_{10}$ cluster is stabilized by oxygen atoms O1, O1A, O3, O3A, O6A, and O6B from BDC ligands. It is of interest that the four water molecules of the cyclic water tetramer in the $(H_2O)_6$ or $(H_2O)_{10}$ clusters are completely coplanar without regard to the connectivity of the hydrogen atoms. The hydrogen-bond lengths are 2.818(4) [OW15–H(15C)···OW16], 2.879(4) [OW15–H(15D)···OW16$^{\#8}$], 2.812(4) [OW2–H(2D)···OW4], and 2.809(4) Å [OW2–H(2C)···OW4$^{\#4}$], and are slightly longer than the average hydrogen-bond length of liquid water tetramer (2.718 Å).[4a,12] In the $(H_2O)_8$ cluster, the lattice water molecules (OW8A, OW8B, OW5, and OW5A) and the coordinated water molecules (OW1 and OW1A) of the $[Cu_2(L)_4(H_2O)_2]^{4+}$ cation are associated by hydrogen bonds to form a cyclic centrosymmetric water hexamer (Figure 2, d). The average OW···OW distance is about 2.80 Å, which is slightly longer than the corresponding value in ice I_h (2.759 Å) and the calculated value of 2.718 Å for cyclic water hexamer.[3] However, they are shorter than those observed in liquid water (2.854 Å).[3] The cyclic water hexamer is hydrogen-bonded to two neighboring water molecules (OW10A and OW10B), yielding a $(H_2O)_8$ cluster. It is worthwhile to note that two water molecules of the $(H_2O)_8$ cluster bind to the Cu^{II} cations. Meanwhile, four water molecules are involved in hydrogen bonds with the oxygen atoms from the carboxylate groups of the

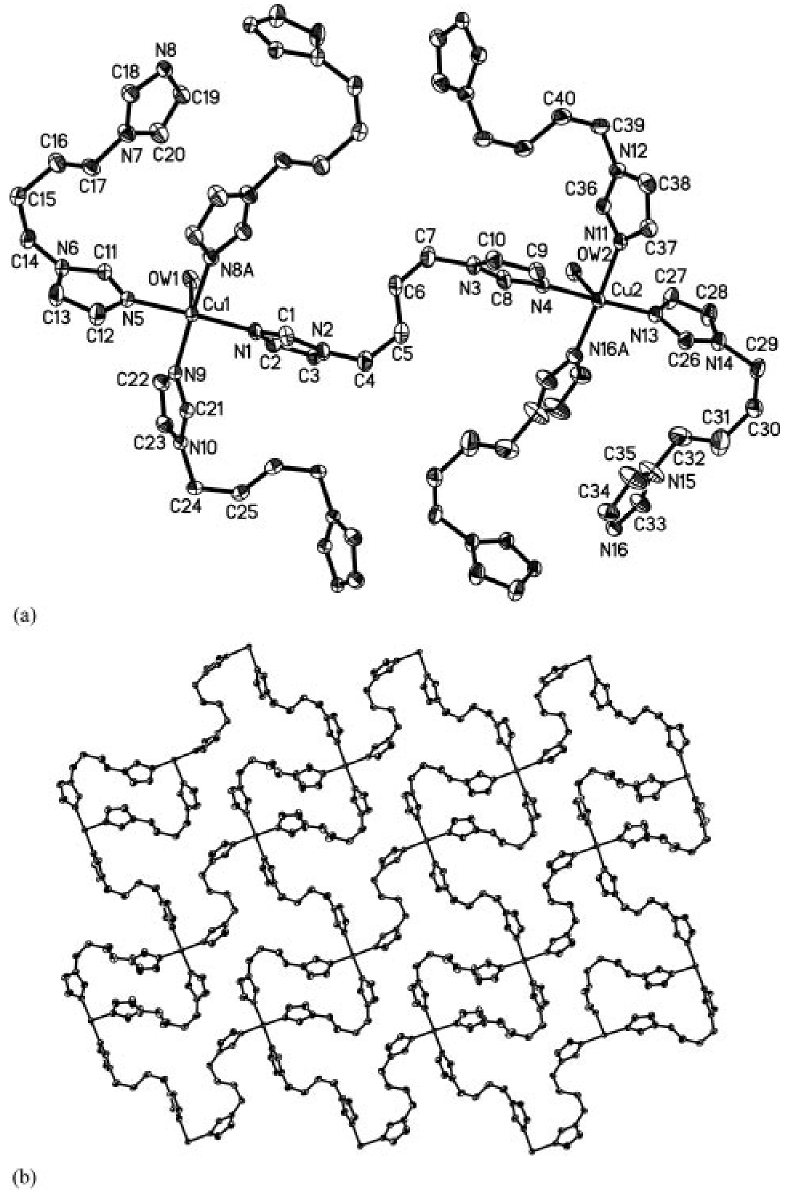

Figure 1. (a) An ORTEP view of complex **1** showing 30% thermal probability ellipsoids. (b) The square-planar, four-connected 2D ${}^{2}_{6}4$ network.

BDC ligands. This indicates that the $(H_2O)_8$ cluster is stabilized not only by hydrogen bonds but also by coordination interactions. The water molecule, the organic BDC anion, and the Cu^{II} cation play a crucial role in the formation of the water clusters. Furthermore, the square-planar, four-connected ${}^{2}_{6}4$ net and the hydrogen-bonded layer are further connected through the coordinating water molecules to form 3D supramolecular structures. Figure 3 (a) displays the packing structure of compound **1**. The H-bonding layers act as a "glue" to reinforce the coordination polymeric ${}^{2}_{6}4$ sheet, forming an overall 3D structure. Each H-bonding layer links two polymeric sheets, and each polymeric sheet is also attached to two H-bonding layers through OW1 and OW2 molecules (Figure 3, b). Here, both water–sheet and water–water interactions are important for the stability of the overall structure.

It should be pointed out that the angles between two neighboring carboxylate groups of BDC and BTC anions are 180° and 120°, respectively, which suggests that the BTC anion may be superior to the BDC anion when it comes to meeting the configurations of $[Cu(L)_n]^{2+}$ (n = 1 or 2) cations, and to coordinate to the Cu^{II} cation (Scheme 1). Thus, during the construction of **2** the multi-carboxylate ligand BTC was chosen as organic anion.

The structure of **2** contains two crystallographically unique Cu^{II} cations, two unique L molecules, and one unique BTC anion. As shown in Figure 4 (a), the Cu1 cation is five-coordinate in a distorted square-pyramidal ge-

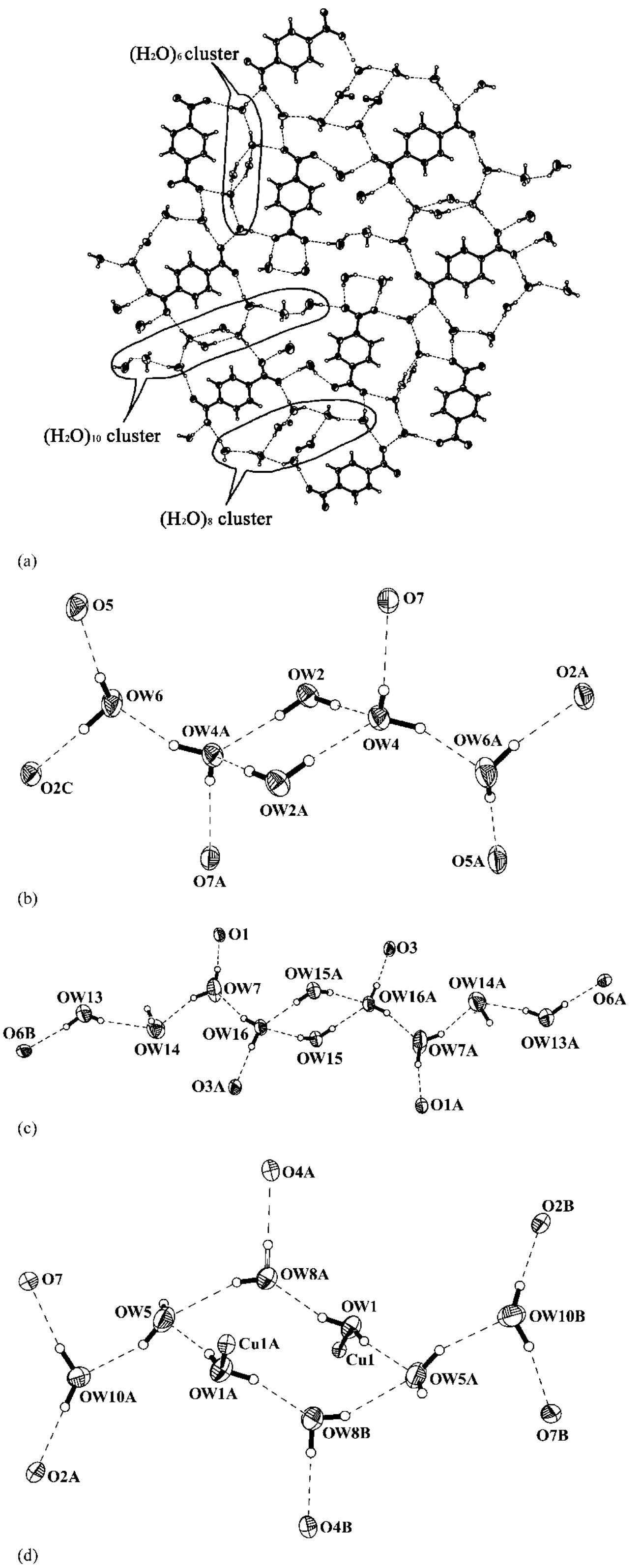

Figure 2. (a) The hydrogen-bonded layer of BDC and water molecules. (b) An ORTEP view showing the $(H_2O)_6$ cluster and its coordination environment. (c) An ORTEP view showing the $(H_2O)_{10}$ cluster and its coordination environment. (d) An ORTEP view showing the $(H_2O)_8$ cluster and its coordination environment.

ometry by coordinating to two nitrogen atoms (N3 and N6A) from two L molecules and three oxygen atoms (O1, O2A, and O3A) from three BTC molecules. The Cu2 center also has a distorted square-pyramidal coordination sphere defined by two carboxylate oxygen atoms (O5 and O5A), one water molecule (OW1), and two nitrogen atoms (N1 and N1A) from two L molecules. The BTC anions bridge the Cu^{II} cations to form 2D networks, which are further connected through the L ligands to form a 3D framework structure, see Figure 4 (b) and Figure 4 (c). In addition, there are some hydrogen-bonded water molecules in the framework of **2**. These water molecules are stabilized by both hydrogen bonds and coordination interactions (OW1 coordinates to Cu2). The hydrogen-bonded water molecules not only fill the voids in the supramolecular framework but also contribute to the total lattice energy. The framework host sufficiently affects the hydrogen bonds of the water molecules and the water molecules maybe also influence the arrangement of the framework host.

If, for reasons of classifying the net, we define the BTC anion as a single point, then it can be considered as a four-connected node (Scheme 1). Thus, there are three kinds of nodes in the structure of **2**: a five-connected node for Cu1, a four-connected node for Cu2, and a four-connected node for the BTC anion. There are some unique four-, six-, eight-, and ten-membered circuits through the nodes in **2** (see Figures S1–S13 in the Supporting Information). For the four-connected BTC anion, each of six sets of links is contained in six-membered circuits (see Figures S1 and S2). Thus, the four-connected BTC anion has the Schäfli symbol 6^6 (Figure 5, a). For the five-connected Cu1 node, ten sets of links are contained in four six-membered circuits (Figures S3–S5), two four-membered circuits (Figure S6), and four eight-membered circuits (Figures S7–10), therefore this node has the Schäfli symbol $(4^2 6^4 8^4)$ (Figure 5, b). For the four-connected Cu2 node, four sets of links are contained in a six-membered circuit (Figure S11), while the other two sets of links are contained in an eight-membered circuit (Figure S12) and a ten-membered circuit (Figure S13), respectively, therefore the four-connected Cu2 node has the Schäfli symbol $(6^4 8 10)$ (Figure 5, c). The molar ratio of these three kinds of nodes is 2:2:1 (BTC/Cu1/Cu2), thus the structure of **2** can be symbolized as a $(6^6)_2(4^2 6^4 8^4)_2(6^4 8 10)$ net with three kinds of nonequivalent points (Figure 5, d).[6] The topological analysis of this net was performed with OLEX.[13] The present case indicates that topological analysis is a useful tool for the description and comparison of natural and artificial networks in crystal engineering.[14]

From the above descriptions, the choice of anion is clearly critical in determining the molecular structures of the final compounds. In this work, both planar two-carboxylate anion and three-carboxylate anion were chosen to study the variation of the structures for **1** and **2**. The topological difference between **1** and **2** should therefore result from the structural features of the BDC and BTC anions. The BDC anion in **1** is not coordinated to the Cu^{II} cation but acts as a counter-anion and template reagent, whereas the BTC anion in **2** meets the configuration of $[Cu(L)_n]^{2+}$

Table 2. Hydrogen-bonding parameters for **1**.[a]

D–H···A [Å]	*d*(D–H) [Å]	*d*(H···A) [Å]	*d*(D···A) [Å]	<(D···H···A) [°]
OW1–H(1D)···OW5$^{\#3}$	0.88(2)	1.93(3)	2.778(4)	161(5)
OW1–H(1C)···OW8$^{\#2}$	0.80(4)	1.98(4)	2.763(4)	166(4)
OW2–H(2D)···OW4	0.879(18)	1.97(2)	2.812(4)	159(4)
OW2–H(2C)···OW4$^{\#4}$	0.87(2)	1.94(2)	2.809(4)	173(5)
OW3–H(3C)···O(4)$^{\#2}$	0.928(17)	1.889(19)	2.805(4)	169(3)
OW3–H(3D)···O(8)	0.868(19)	1.99(2)	2.850(4)	168(4)
OW4–H(4D)···O(7)	0.88(2)	1.89(2)	2.740(4)	163(4)
OW4–H(4C)···OW6$^{\#4}$	0.84(4)	1.90(4)	2.719(4)	165(4)
OW5–H(5D)···OW10$^{\#5}$	0.896(18)	2.01(3)	2.827(4)	151(3)
OW6–H(6D)···O(2)$^{\#1}$	0.901(18)	1.91(2)	2.750(4)	154(3)
OW6–H(6C)···O(5)	0.871(18)	1.91(2)	2.780(4)	172(3)
OW7–H(7C)···O(1)	0.888(18)	1.95(2)	2.816(4)	165(4)
OW7–H(7D)···OW14	0.842(18)	2.208(16)	2.763(5)	123(2)
OW8–H(8C)···O(4)	0.875(19)	1.90(2)	2.767(4)	174(5)
OW8–H(8D)···OW5$^{\#2}$	0.90(4)	2.03(2)	2.849(4)	151(4)
OW9–H(9C)···O(3)	0.825(18)	1.99(3)	2.702(4)	144(3)
OW10–H(10D)···O(2)	0.90(4)	1.88(4)	2.779(4)	170(3)
OW10–H(10C)···O(7)$^{\#7}$	0.896(18)	1.98(2)	2.851(4)	164(3)
OW11–H(11D)···O(5)$^{\#1}$	0.92(4)	1.78(2)	2.693(4)	176(5)
OW12–H(12C)···O(6)$^{\#1}$	0.83(5)	2.01(5)	2.812(4)	163(5)
OW12–H(12D)···OW11	0.90(2)	2.17(5)	2.837(4)	131(5)
OW13–H(13D)···O(6)$^{\#8}$	0.866(19)	1.88(3)	2.713(4)	161(6)
OW13–H(13C)···OW14	0.999(18)	2.134(15)	2.791(5)	122(4)
OW15–H(15C)···OW16	0.874(19)	1.95(2)	2.818(4)	174(4)
OW15–H(15D)···OW16$^{\#6}$	0.858(18)	2.04(2)	2.879(4)	167(3)
OW16–H(16D)···O(3)	0.89(4)	1.89(2)	2.773(4)	175(4)
OW16–H(16C)···OW7$^{\#6}$	0.89(4)	1.82(2)	2.672(4)	163(4)

[a] Symmetry transformations used to generate equivalent atoms: $^{\#1}$ $-x+1, -y, -z$; $^{\#2}$ $-x+1, -y, -z-1$; $^{\#3}$ $-x, -y, -z-1$; $^{\#4}$ $-x, -y, -z$; $^{\#5}$ $x-1, y, z$; $^{\#6}$ $-x+1, -y+1, -z-1$; $^{\#7}$ $x+1, y, z$; $^{\#8}$ $x, y+1, z$.

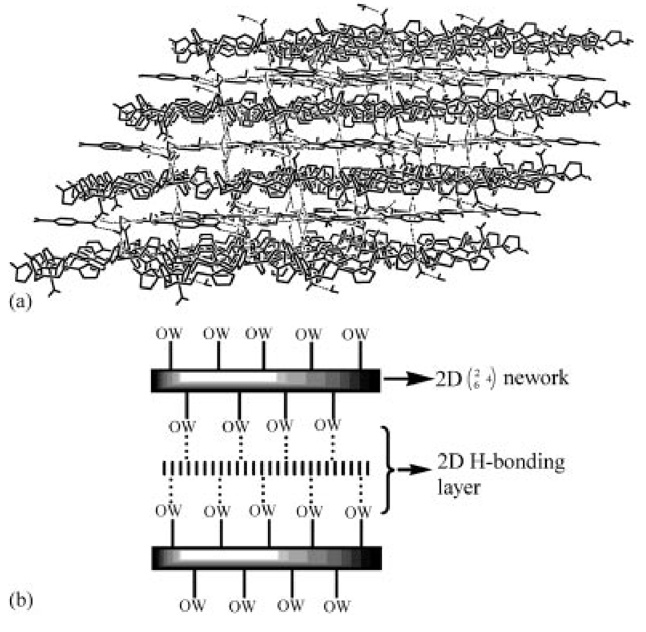

Figure 3. (a) The 3D H-bonding structure of **1**. (b) A schematic representation of the 3D H-bonding structure.

($n = 1$ or 2) cations and coordinates to the Cu^{II} cation as a four-coordinate ligand. Although different Cu/L ratios (1:1, 1:2, 1:3, and 1:4) were used in the preparations, only **1** and **2** were isolated as the products. Thus, the formation of these different frameworks is due to the effects of different organic anions.

IR Spectra and TGA

The solid-state IR spectra of **1** and **2** in the region 4000–400 cm^{-1} exhibit characteristic bands for BDC, BTC, and L ligands (see Figure S14 in the Supporting Information). The IR spectrum of **1** shows a broad band centered around 3427 cm^{-1} attributable to the O–H stretching frequency of the water cluster. The IR spectrum of ice shows the O–H stretch at 3220 cm^{-1}, while this stretching vibration in liquid water appears at 3490 and 3280 cm^{-1}.[15] This indicates that the water cluster in **1** has an O–H stretching vibration similar to that of liquid water, and the slight difference is attributable to the environment that the clusters are in.[16] The peaks around 1600, 1560, 1400, and 1350 cm^{-1} for **1** and **2** can be attributed to the asymmetric and symmetric vibrations of the carboxylate groups.[17]

In order to characterize the compounds **1** and **2** more fully in terms of thermal stability, we studied them by TGA. Compounds **1** and **2** were heated from 35 to 780 °C under N_2. As expected, the TGA curves of compounds **1** and **2** exhibit three similar weight-loss stages. The first weight loss, corresponding to the water molecules, is observed over the wide temperature range 35–90 °C (observed 18.6%, calculated 19.1%) for **1** and 35–93 °C (observed 6.7%, calculated 7.1%) for **2**. The second weight loss is 52.4% (calculated 50.6%) for **1** in the range 238–350 °C and 46.4% (calculated 45.1%) for **2** in the range 239–344 °C, and is assigned to the release of L molecules. Drastic weight losses corre-

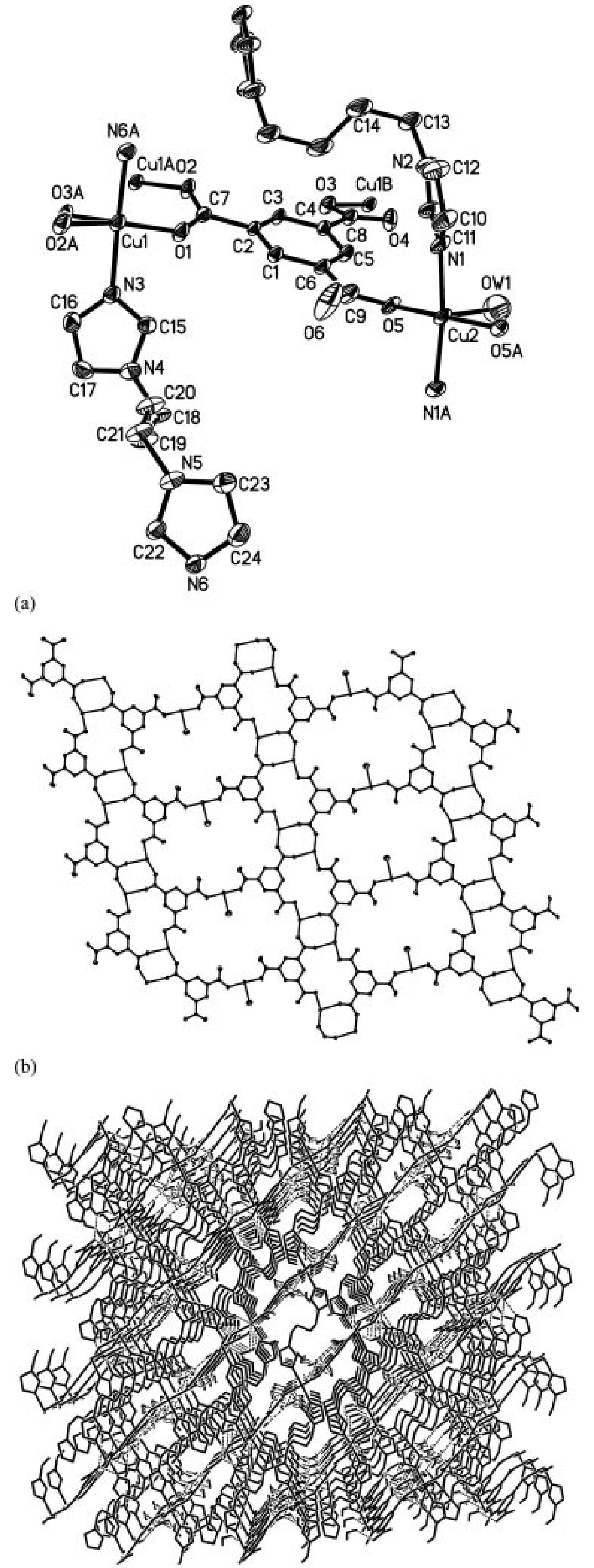

Figure 4. (a) ORTEP view of **2** showing 30% thermal probability ellipsoids. (b) The 2D layered structure constructed by BTC and Cu^{II} cations. (c) The packing diagram of **2**.

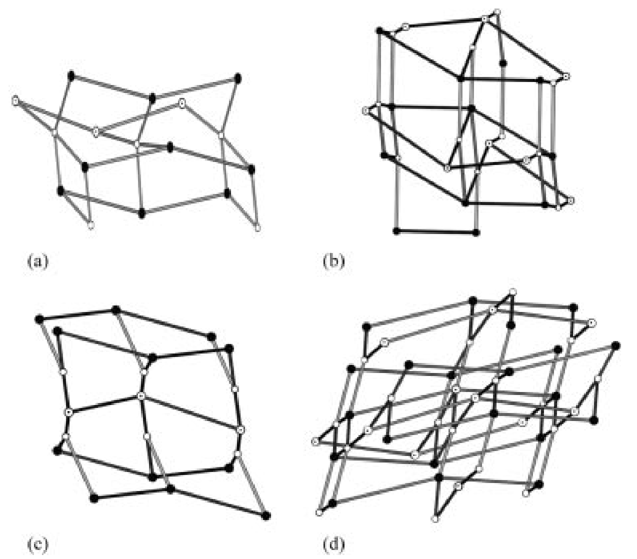

Figure 5. (a) Schematic representation of the circuits through the four-connected BTC node. (b) Schematic representation of the circuits through the five-connected Cu1 node. (c) Schematic representation of the circuits through the four-connected Cu2 node. (d) The $(6^{6})_{2}(4^{2}6^{4}8^{4})_{2}(6^{4}810)$ net with three kinds of nonequivalent points. (Cu2 = ⊙, BTC = ○, Cu1 = ●).

sponding to the removal of BDC and BTC were observed from 420 to 528 °C for **1** and from 423 to 524 °C for **2**, respectively.

Conclusions

Two new Cu^{II} coordination polymers with different topologies have been obtained due to the effects of different organic anions on the final frameworks' formation. When the BDC anion was chosen as the dicarboxylate anion, a coordination polymer **1** with an unusual, square-planar, four-connected ${}^{2}_{6}4$ net and three types of water clusters was obtained. In **2**, the BTC anion coordinates to the Cu^{II} cation as a tetradentate ligand to form a $(6^{6})_{2}(4^{2}6^{4}8^{4})_{2}(6^{4}810)$ net with three kinds of nonequivalent points.

Experimental Section

Materials and Methods: All reagents and solvents for syntheses were purchased from commercial sources and used as received. A Perkin–Elmer 240 elemental analyzer was used to collect microanalytical data, and the FT-IR spectrum was recorded from KBr pellets in the range 4000–400 cm^{-1} on a Mattson Alpha-Centauri spectrometer. TGA was performed with a Perkin–Elmer TG-7 analyzer under nitrogen.

Synthesis of 1,1′-(1,4-Butanediyl)bis(imidazole) (L): A mixture of imidazole (3.4 g, 50 mmol) and NaOH (2.0 g, 50 mmol) in DMSO (10 mL) was stirred at 60 °C for 1 h, and then 1,4-dichlorobutane (3.2 g, 25 mmol) was added. The mixture was cooled to room temperature after stirring at 60 °C for 2 h and then poured into 200 mL of water. A white solid formed immediately, which was isolated by filtration in 86% yield (4.1 g) after drying in air. $C_{10}H_{14}N_4$ (190.25): calcd. C 63.16, H 7.37, N 29.47; found C 63.11, H 7.42, N 29.31.

Synthesis of $[Cu_2(L)_4(H_2O)_2]\cdot(BDC)_2\cdot 14H_2O$ (1): A mixture of $CuCl_2\cdot 2H_2O$ (0.171 g, 1 mmol), NaOH (0.080 g, 2 mmol), and H_2BDC (0.166 g, 1 mmol) in water was stirred for 10 min at 60 °C, then 1,1′-(1,4-butanediyl)bis(imidazole) (L; 0.190 g, 1 mmol) was added to the mixture. After stirring for 30 min, the blue precipitate was collected and dissolved in a minimum amount of ammonia (14 M). Suitable blue single crystals of **1** were obtained by slow evaporation of this solution at ambient temperature in 73% yield (109.8 mg). $C_{56}H_{96}Cu_2N_{16}O_{24}$ (1504.6): calcd. C 44.66, H 6.38, N 14.89; found C 44.89, H 6.60, N 14.49.

Synthesis of $[Cu_{1.5}(BTC)(L)_{1.5}(H_2O)_{0.5}]\cdot 2H_2O$ (2): Compound **2** was prepared in the same way as for **1**, but with 1,3,5-benzenetricarboxylic acid (H_3BTC), in 53% yield (33.5 mg). $C_{24}H_{29}Cu_{1.5}N_6O_{8.5}$ (632.84): calcd. C 45.51, H 4.58, N 13.27; found C 45.22, H 4.51, N 13.79.

X-ray Crystallography: Single-crystal X-ray diffraction data for complexes **1** and **2** were recorded with a Rigaku RAXIS-RAPID image plate diffractometer and a Bruker-AXS Smart CCD diffractometer, respectively, using the ω-scan technique with Mo-K_α radiation (λ = 0.71073 Å). All the structures were solved by direct methods with SHELXS-97[18] and refined by full-matrix least-squares techniques using the SHELXL-97 program.[19] Non-hydrogen atoms were refined with anisotropic temperature parameters the and the hydrogen atoms of the ligands were refined as rigid groups. The hydrogen atoms of the water molecules for **1** and **2** were located from the difference Fourier maps. Further details of the structural analysis are summarized in Table 3.

Table 3. Summary of X-ray crystallographic data for compounds **1** and **2**.

Compound	**1**	**2**
Formula	$C_{56}H_{96}Cu_2N_{16}O_{24}$	$C_{24}H_{29}Cu_{1.5}N_6O_{8.5}$
Mol. mass	1504.57	632.84
Space group	$P\bar{1}$	$C2/c$
a [Å]	13.049(3)	25.860(6)
b [Å]	13.334(3)	10.185(2)
c [Å]	21.562(4)	22.790(5)
α [°]	91.46(3)	90
β [°]	101.60(3)	97.671(7)
γ [°]	99.41(3)	90
V [Å^3]	3619.2(13)	5949(2)
Z, $d_{calcd.}$ [g cm^{-3}]	2, 1.381	8, 1.413
μ (Mo-K_α [mm^{-1}])	0.672	1.137
$F(000)$	1588	2612
Reflns. collected / unique	29446 / 14091	18017 / 7010
Reflns. obsd. [$I > 2\sigma(I)$]	8141	3181
GOF on F^2	0.940	0.885
$R1$,[a] $wR2$[b] (obsd.)	0.0462, 0.1260	0.0633, 0.1237
(Δ/σ) max., mean	0.001, 0.000	0.001, 0.000
Max., min. peaks [e Å^{-3}]	0.541, –0.607	0.858, –0.324

[a] $R1 = \Sigma||F_o| - |F_c||/\Sigma|F_o|$. [b] $wR2 = |\Sigma w(|F_o|2 - |F_c|2)|/\Sigma|w(F_o)^2|^{1/2}$, where $w = 1/[\sigma^2(F_o^2) + (aP)^2 + bP]$ and $P = (F_o^2 + 2F_c^2)/3$.

CCDC-216567 (for **1**) and -281108 (for **2**) and contain the supplementary crystallographic data for this paper. These data can be obtained free of charge from The Cambridge Crystallographic Data Centre via www.ccdc.cam.ac.uk/data_request/cif.

Supporting Information (see footnote on the first page of this article): Figures of circuits around the nodes for **2** (Figures S1–S13). The IR spectra of compounds **1** and **2** (Figure S14).

Acknowledgments

We thank the National Natural Science Foundation of China (no. 20471014), the Fok Ying Tung Education Foundation, and the Natural Science Foundation of Jilin province (China) for financial support.

---

[1] a) G. A. Jeffrey, *An Introduction to Hydrogen Bonding*, Oxford University Press, Oxford, U.K., **1997**, pp. 160–180; b) A. L. Gillon, N. Feeder, R. J. Davey, R. Storey, *Cryst. Growth Des.* **2003**, *3*, 663–673; c) R. Ludwig, *Angew. Chem. Int. Ed.* **2001**, *40*, 1808–1827.

[2] a) B.-Q. Ma, H.-L. Sun, S. Gao, *Angew. Chem. Int. Ed.* **2004**, *43*, 1374–1376; b) S. W. Benson, E. D. Siebert, *J. Am. Chem. Soc.* **1992**, *114*, 4269–4276; c) K. A. Udachin, J. A. Ripmeester, *Nature* **1999**, *397*, 420–423; d) B.-H. Ye, B.-B. Ding, Y.-Q. Weng, X.-M. Chen, *Inorg. Chem.* **2004**, *43*, 6866–6868; e) N. S. Oxtoby, A. J. Blake, N. R. Champness, C. Wilson, *Chem. Eur. J.* **2005**, *11*, 1–13.

[3] D. Eisenberg, W. Kauzmann, *The Structure and Properties of Water*, Oxford University Press, Oxford, U.K., **1969**.

[4] a) J. D. Cruzan, L. B. Braly, K. Liu, M. G. Brown, J. G. Loeser, R. J. Saykally, *Science* **1996**, *271*, 59–62; b) B. Zhao, P. Cheng, X. Chen, C. Cheng, W. Shi, D. Liao, S. Yan, Z. Jiang, *J. Am. Chem. Soc.* **2004**, *126*, 3012–3013; c) S. K. Ghosh, P. K. Bharadwaj, *Inorg. Chem.* **2003**, *42*, 8250; d) S. K. Ghosh, P. K. Bharadwaj, *Angew. Chem. Int. Ed.* **2004**, *43*, 3577–3580.

[5] a) S. Leininger, B. Olenyuk, P. J. Stang, *Chem. Rev.* **2000**, *100*, 853–908; b) S. R. Batten, R. Robson, *Angew. Chem. Int. Ed.* **1998**, *37*, 1460–1494; c) B. Moulton, M. J. Zaworotko, *Chem. Rev.* **2001**, *101*, 1629–1658; d) S.-I. Noro, R. Kitaura, M. Kondo, S. Kitagawa, T. Ishii, H. Matsuzaka, M. Yamashita, *J. Am. Chem. Soc.* **2002**, *124*, 2568–2583; e) L. Carlucci, G. Ciani, D. M. Proserpio, *Coord. Chem. Rev.* **2003**, *246*, 247–289; f) D.-L. Long, R. J. Hill, A. J. Blake, N. R. Champness, P. Hubberstey, D. M. Proserpio, C. Wilson, M. Schröder, *Angew. Chem. Int. Ed.* **2004**, *43*, 1851–1854; g) M.-L. Tong, X.-M. Chen, S. R. Batten, *J. Am. Chem. Soc.* **2003**, *125*, 16170–16171; h) L. Carlucci, G. Ciani, D. M. Proserpio, *Chem. Commun.* **2004**, 380–381.

[6] a) A. F. Wells, *Three-Dimensional Nets and Polyhedra*, Wiley-Interscience, New York, **1977**; b) A. F. Wells, *Further Studies of Three-Dimensional Nets*; ACA Monograph 8, American Crystallographic Association, **1979**.

[7] a) P. J. Hagrman, D. Hagrman, J. Zubieta, *Angew. Chem. Int. Ed.* **1999**, *38*, 2638–2684; b) Z.-R. Qu, H. Zhao, Y.-P. Wang, X.-S. Wang, Q. Ye, Y.-H. Li, R.-G. Xiong, B. F. Abrahams, Z.-G. Liu, Z.-L. Xue, X.-Z. You, *Chem. Eur. J.* **2004**, *10*, 53–60; c) T. M. Reineke, M. Eddaoudi, M. O'Keeffe, O. M. Yaghi, *Angew. Chem. Int. Ed.* **1999**, *38*, 2590–2594.

[8] a) J.-F. Ma, J.-F. Liu, Y. Xing, H.-Q. Jia, Y.-H. Lin, *J. Chem. Soc., Dalton Trans.* **2000**, 2403–2407; b) J.-F. Ma, J.-F. Liu, Y.-C. Liu, Y. Xing, H.-Q. Jia, Y.-H. Lin, *New J. Chem.* **2000**, *24*, 759–763; c) J.-F. Ma, J. Yang, G.-L. Zheng, L. Li, J.-F. Liu, *Inorg. Chem.* **2003**, *42*, 7531–7534; d) J. Yang, J.-F. Ma, Y.-Y. Liu, S.-L. Li, G.-L. Zheng, *Eur. J. Inorg. Chem.* **2005**, 2174–2180.

[9] a) X.-H. Bu, M.-L. Tong, H. C. Chang, S. Kitagawa, S. R. Batten, *Angew. Chem. Int. Ed.* **2004**, *43*, 192–195; b) J.-P. Zhang, S.-L. Zheng, X.-C. Huang, X.-M. Chen, *Angew. Chem. Int. Ed.* **2004**, *43*, 206–209.

[10] S. Supriya, S. K. Das, *New J. Chem.* **2003**, *27*, 1568–1574.

[11] J. Tao, Z.-J. Ma, R.-B. Huang, L.-S. Zheng, *Inorg. Chem.* **2004**, *43*, 6133–6135.

[12] A. Geiger, P. Mausbach, J. Schnitker, *Water and Aqueous Solutions*, Hilger, Bristol, **1986**, p. 15.

[13] O. V. Dolomanov, A. J. Blake, N. R. Champness, M. Schröder, *J. Appl. Crystallogr.* **2003**, *36*, 1283–1284.

[14] C.-Y. Su, M. D. Smith, A. M. Goforth, H.-C. zur Loye, *Inorg. Chem.* **2004**, *43*, 6881–6883.
[15] R. Custelcean, C. Afloroaei, M. Vlassa, M. Polverejan, *Angew. Chem. Int. Ed.* **2000**, *39*, 3094–3096.
[16] a) S. Neogi, P. K. Bharadwaj, *Inorg. Chem.* **2005**, *44*, 816–818; b) S. K. Ghosh, P. K. Bharadwaj, *Inorg. Chem.* **2004**, *43*, 6887–6889.
[17] J.-F. Ma, J. Yang, S.-L. Li, S.-Y. Song, H.-J. Zhang, H.-S. Wang, K.-Y. Yang, *Cryst. Growth Des.* **2005**, *5*, 807–812.
[18] G. M. Sheldrick, *SHELXS-97, Programs for X-ray Crystal Structure Solution*; University of Göttingen, Germany, **1997**.
[19] G. M. Sheldrick, *SHELXL-97, Programs for X-ray Crystal Structure Refinement*; University of Göttingen, Germany, **1997**.

Received: August 18, 2005